Research Article Vol. 10, No. 7 | 1 Jul 2019 | BIOMEDICAL OPTICS EXPRESS 3343

Biomedical Optics EXPRESS

GCaMP6 ΔF/F dependence on the excitation wavelength in 3-photon and 2-photon microscopy of mouse brain activity

DIMITRE G. OUZOUNOV,* TIANYU WANG, CHUNYAN WU, AND CHRIS XU

School of Applied and Engineering Physics, Cornell, Ithaca, NY 14850, USA
**ouzounov@cornell.edu*

Abstract: A fundamental challenge in calcium imaging is to minimize the excitation laser power while still maintaining a sufficient signal-to-noise ratio to distinguish individual transients in the fluorescence traces. It is important to characterize relative fluorescence (i.e., ΔF/F) dependence on the excitation wavelength *in vivo* where the environment cannot be controlled effectively during imaging. Leveraging time division multiplexing of two excitation beams to achieve nearly simultaneous 2-photon and 3-photon imaging of the calcium transients, we measured systematically the ΔF/F dependence on the excitation wavelength in 2-photon and 3-photon *in vivo* imaging of neuronal activity in mouse brain labeled with GCaMP6s. The technique can be applied to *in vivo* measurements of other fluorescence sensors.

1. Introduction

Fluorescence microscopy together with a variety of fluorescent indicators are routinely used to visualize activity of a single cell as well as to record neuronal circuits *in vivo* [1,2]. Since its inception, two-photon fluorescence microscopy (2PM) [3,4] has become the key method for structural and functional imaging of populations of neurons *in vivo* [5–10]. Three-photon fluorescence microscopy (3PM) [11–14] has been demonstrated recently to extend the depth limit of 2PM and to allow neuronal activity imaging with high spatial and temporal resolution deep into scattering brain tissue *in vivo*. Ultrasensitive genetically-encoded calcium sensors have been developed and demonstrated [15,16].

Neuronal activities lead to fast transients in the concentration of intracellular free calcium. GCaMP6 protein indicators respond to Ca2 + changes with large change in fluorescence intensity, and are used routinely to image the activity of cells [17]. The action potentials are visualized as transients in the fluorescence emission, and the goal of any optical technique is to image these transients with minimal excitation power. Therefore, it is important to find the imaging conditions that maximize the Ca-dependent contrast of fluorescence intensity.

The large dynamic range of fluorescence emission of GCaMP6 upon binding with calcium is mainly due to redistribution of the chromophore from neutral to anionic form, which is the origin of almost all fluorescence emission [18]. Because the neutral and anionic form of GCaMP6 have different absorption and fluorescence excitation spectra, the relative fluorescence change (i.e., ΔF/F) of GCaMP6 upon binding to calcium ion depends strongly on the excitation wavelength. The acidity level (pH factor) of the environment also affects significantly the anionic chromophore concentration and thus the amount of fluorescence.

Most of the calcium imaging of neural activity has been performed using two-photon excitation, however, systematic study *in vivo* on the optimal excitation wavelength has not been reported. GCaMP6 single photon excitation spectrum has been measured and reported but one-photon (1p) absorption properties do not determine the two-photon (2p) and three-photon (3p) absorption properties.

#361282 https://doi.org/10.1364/BOE.10.003343
Journal © 2019 Received 6 Mar 2019; revised 4 May 2019; accepted 29 May 2019; published 14 Jun 2019

For many well-known fluorophores, one-photon absorption (1PA) spectrum cannot predict the two-photon absorption (2PA) spectrum because the selection rule for 2PA is different from that for 1PA [4]. On the other hand, the selection rule for three-photon absorption (3PA) and 1PA is the same, and it has been shown that 3PA spectrum follows closely the corresponding 1PA for some fluorophores [19]. Recent measurements of several fluorophores at the long wavelength spectral range of ~1700 nm, however, showed marked difference between the 3PA and 1PA spectra [20], indicating that the 1PA spectrum cannot predict the 3PA spectrum for some fluorophores. More systematic studies are needed to further elucidate this phenomenon.

1p and 2p excitation spectra for purified GCaMP6 proteins have been measured for Ca-free and Ca-saturated states *ex vivo* [18]. Although, these results are illuminating, they were achieved in a very well controlled environment: Ca-free or Ca-saturated. In addition, the pH was set to optimize fluorescence but the optimal value is not necessarily close to physiological pH of the brain. All these parameters are difficult to control in *in vivo* imaging. It is important that systematic measurements are performed *in vivo* to determine the optimal excitation wavelength for 2PM and 3PM that provides maximum Ca-dependent contrast of fluorescence intensity, and thus enable imaging with the highest transient detection fidelity with the lowest excitation power.

2. Experimental setup

Investigating the dependence of the ΔF/F on the excitation wavelength *in vivo* is challenging because it is impossible to maintain exactly the same neural activity in a live animal when imaging repeatedly at various wavelengths of interest, even for the same neuron and under the same stimulation. To overcome this hurdle, we developed a time division multiplexing (TDM) technique for nearly simultaneous imaging of the same transients train with 2p and 3p excitation [12]. A 2p excitation beam and a 3p excitation beam are first spatially overlapped to have the same focal position after the objective. The 2p excitation pulse train is only switched on between two adjacent pulses of the 3p excitation for about one microsecond. Therefore, the sample is alternately excited by 2p absorption and 3p absorption within the microsecond time scale (i.e., nearly simultaneous). Recording of the 3p pulse train allows to separate 2- and 3-photon excited fluorescence in post processing analysis of the recorded images.

A noncollinear optical parametric amplifier (NOPA, Spectra Physics) pumped by a regenerative amplifier (Spirit, Spectra Physics) was used as the excitation source for 3PM. A two-prism (SF11 glass) compressor is used to compensate for the normal dispersion of the optics of the light source and the microscope, including the objective. For this study, the NOPA was operated in the wavelength range from 1250 nm to 1400 nm. The average power of the NOPA at any wavelength of operation was ~500 mW (1250 nJ per pulse at 400 kHz repetition rate) and the spectral bandwidth was 70-80 nm. A set of bandpass filters (Edmund optics, #87-828, #87-829, #87-830, #87-831) was used to narrow the spectral width of the excitation light to 25 nm. The original pulse duration (measured by second-order interferometric autocorrelation) under the objective is ~55 fs after adjusting the prism compressor. After filtering the spectrum, a typical pulse duration under objective was measured to be ~120 fs. While the shorter, 55-fs pulse is preferred for 3PM, the narrower spectral bandwidth after filtering allows us to measure the wavelength dependence of ΔF/F more precisely.

The excitation source for 2PM is a mode-locked Ti:Sapphire laser (Tsunami, Spectra Physics). In this study, the wavelength was tuned from 880 nm to 950 nm. The output of the Ti:sapphire laser is modulated with an electro-optical modulator (Conoptics, model 350-160), which is capable of sub-μs intensity modulation. The 2p and 3p beams are combined by a dichroic mirror (DM), spatially overlapped, and directed to the microscope (Fig. 1).

Biomedical Optics EXPRESS

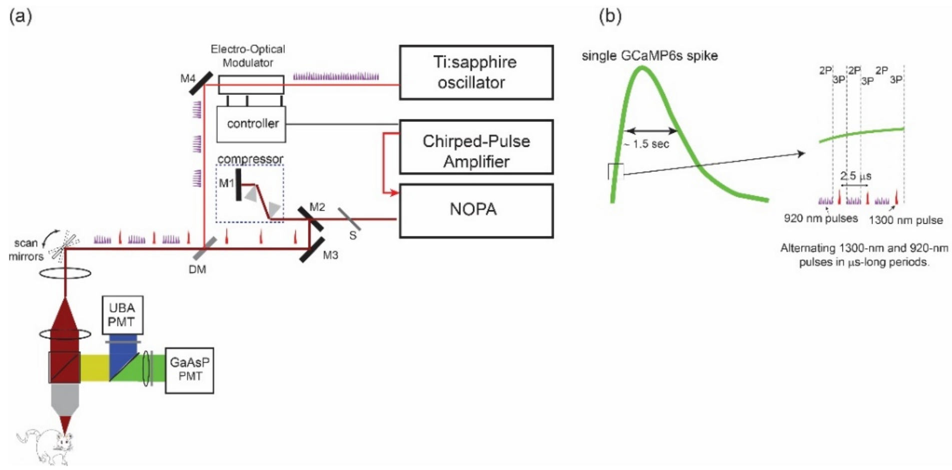

Fig. 1. (a) Schematic illustration of the imaging setup. (b) Time division multiplexing for near-simultaneous 2PM and 3PM of the same brain activity.

The axial width of the point spread functions for both beams and their spatial overlap was measured by imaging fluorescent beads for all 3p excitation wavelengths (1250 nm – 1375 nm) and for 2p excitation wavelength of 920. During the *in vivo* imaging experiments, only the wavelength of the NOPA was tuned, and no other adjustments were made on the optical beam path. The excitation focal volumes for both beams have similar axial width (within ~10%), and nearly perfect overlap in the axial direction for all wavelengths. Typical result is shown in Fig. 2(d).

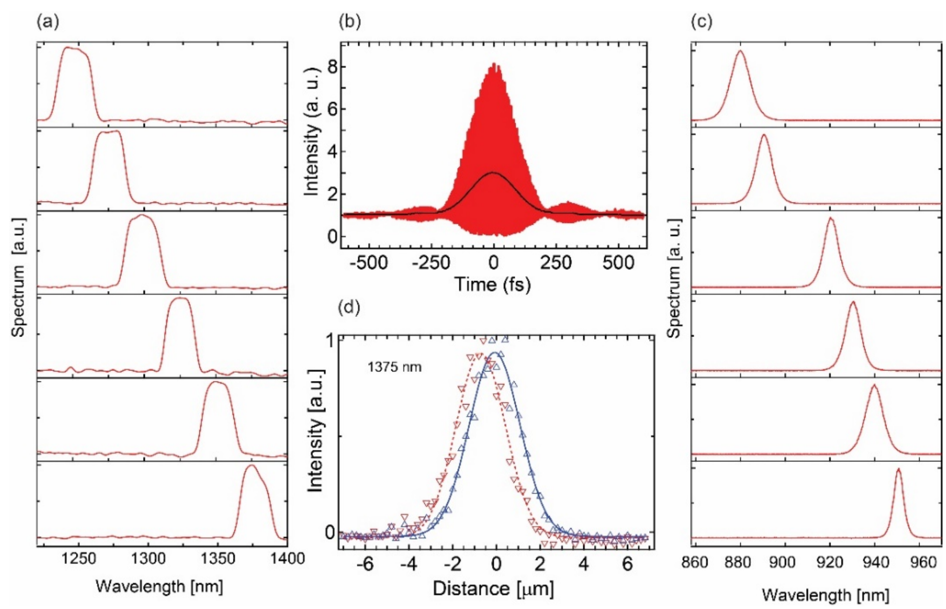

Fig. 2. Characterization of the excitation sources. (a) NOPA output spectrum at various wavelengths filtered with a bandpass filter with 25-nm bandwidth. (b) Typical autocorrelation trace of the NOPA output pulse after spectral filtering. (c) Two-photon excitation spectrum at various wavelengths. (d) 2p (blue) and 3p (red) axial scan of a fluorescent bead showing the similar axial resolution and the overlap of the focal volumes of the two excitation beams. The triangles are the measured data and the solid lines are the Gaussian fittings to the measurements.

The imaging setup is described in detail in [12]. In brief, we used a custom-built multiphoton laser scanning microscope with a high numerical aperture objective (Olympus XLPLN25XWMP2, 25X, NA 1.05). The fluorescence and harmonic generation signals are epi-collected through the objective and directed onto the photomultiplier tubes (PMTs) by a dichroic beamspliter (FF705-Di01-25x36, Semrock). Our system has two detection channels for the fluorescence signal from the calcium sensor and for the third harmonic generation (THG) signal generated at various interfaces. The animal is placed on a motorized stage, and the whole imaging setup is controlled by ScanImage 3.8.

We recorded spontaneous activity traces in an awake mouse with 2PM and 3PM simultaneously from the same neuron. While keeping constant one of the excitation wavelengths (e.g., 2PM at 920 nm), we varied the wavelength of the other beam (e.g., 3PM from 1250 nm to 1400 nm). We imaged the neuron continuously using 60μmx30μm field of view at 13.6 Hz frame rate in a series of movies of ~75 second each. The power after the objective lens was 2-3 mW for 3PM and 5-6 mW for 2PM. Tuning one of the excitation wavelength resulted in a small lateral displacement of the image (~1 micron), which is not an issue because the multiplexed images are separated in the time domain and analyzed independently in the post-processing stage.

3. Results

To determine the $\Delta F/F_0$dependence on the excitation wavelength in 3PM and 2PM, we used the TDM technique described above to image spontaneous brain activity in cortical layer 2/3 neurons in awake transgenic mice (CamKII-tTA/GCaMP6s, male, 20 and 31 weeks old). Cranial window was implanted to image a site located approximately 2 mm posterior and 2.5 mm lateral to the Bregma point. The same neurons were imaged with 2PM at excitation wavelength 920 nm and with 3PM at excitation wavelength varied between 1250 and 1375 nm. In Fig. 3(a), we show high resolution 3p image of the area where the activity traces were recorded. Figure 3(b) shows the same neuron imaged by 2PM and 3PM using the TDM technique. In Fig. 3(c), we plot examples of activity traces recorded using 2PM at 920-nm excitation wavelength and 3PM at various excitation wavelengths. It is clearly seen that the 3p excited $\Delta F/F$ is the smallest at the excitation wavelength of 1250 nm and becomes larger with longer excitation wavelengths. We quantify this dependence by calculating the ratio of the 3p excited trace and the 2p excited trace recorded at the same time from the same neuron (Fig. 3(a)). The results are shown in Fig. 3(c).

Biomedical Optics EXPRESS

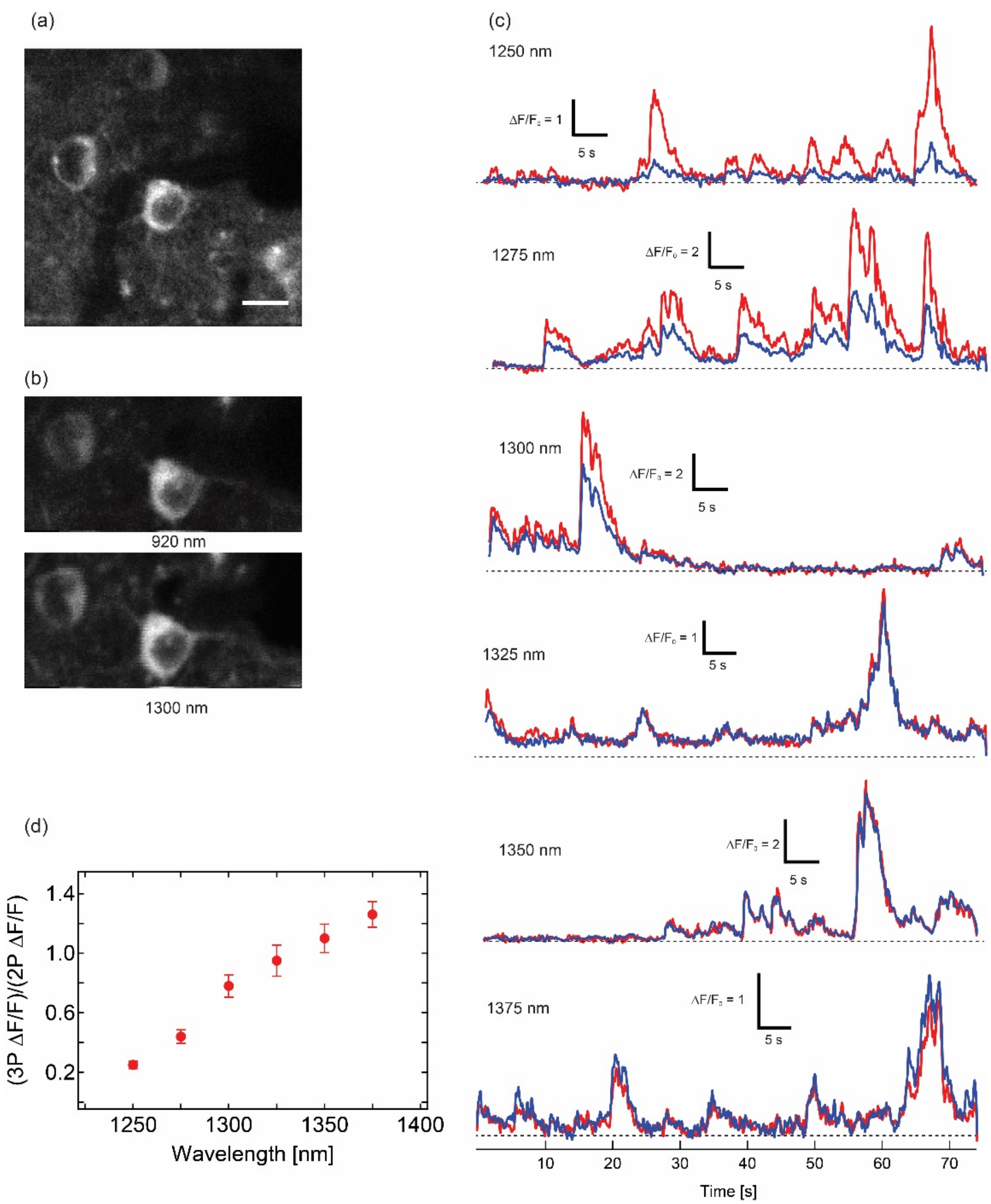

Fig. 3. Three-photon-excited relative fluorescence versus the excitation wavelength. (a) High resolution 3p image of the region where the traces were recorded. Scale bar, 10 µm. (b) Near-simultaneous 2p (top) and 3p (bottom) imaging of GCaMP6s-labeled neurons in transgenic mouse (CamKII-tTA/tetO-GCaMP6s) cortex at depth of ~250 um. (c) Activity trace of the neuron in (a) recorded. Two-photon activity traces (red) are recorded at excitation wavelength of 920 nm. Three-photon activity traces (blue) are recorded at various excitation wavelengths as indicated. All traces are recoded with the same neuron. Tuning the 3p excitation wavelength slightly changes the transverse position of the 3P image (~one micron). (d) Ratio of three-photon excited relative fluorescence at various excitation wavelengths and two-photon excited relative fluorescence at 920-nm excitation wavelength. Each ratio and its variation are calculated from the recorded 2p and 3p traces over 430 – 510 seconds.

We further investigate systematically the dependence of two-photon excited ΔF/F on the excitation wavelength. The three-photon excitation wavelength was now kept constant at

Biomedical Optics EXPRESS

1310 nm while the two-photon excitation wavelength was tuned from 880 nm to 950 nm (Fig. 4(a)). Examples of activity traces recorded with 3PM and 2PM are shown in Fig. 4(b). The ratios of 2p-excited ΔF/F at various excitation wavelengths to 3p-excited ΔF/F at 1310 nm are shown in Fig. 4(c).

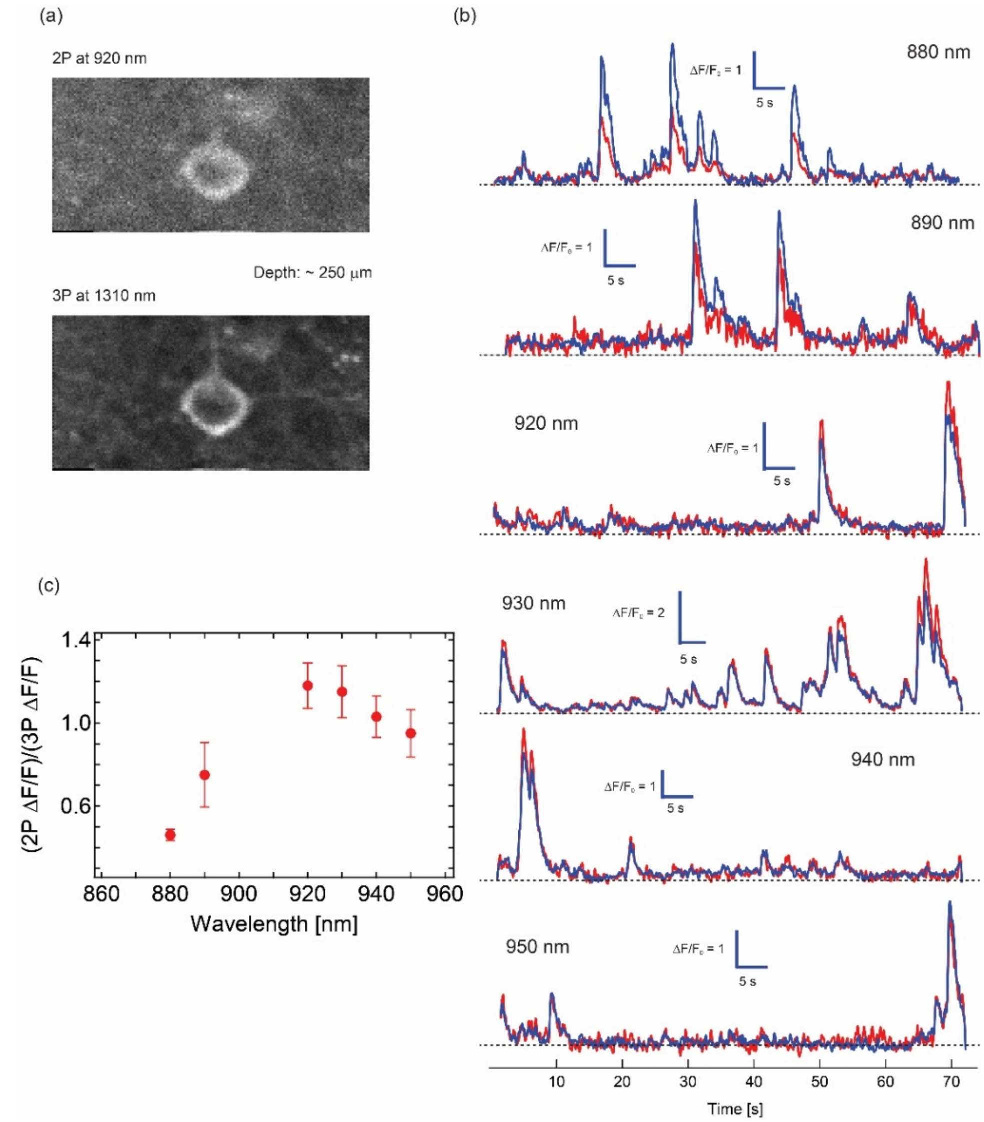

Fig. 4. Two-photon-excited relative fluorescence versus the excitation wavelength. (a) Near-simultaneous 2P (top panel) and 3P (bottom panel) imaging of GCaMP6s-labeled neurons in transgenic mouse (CamKII-tTA/tetO-GCaMP6s) cortex at depth of ~250 um. (b) Activity trace of the neuron in (a) recorded. Three-photon activity traces (blue) are recorded at excitation wavelength of 1310 nm. Two-photon activity traces (red) are recorded at various excitation wavelengths as indicated. All traces are recoded with the same neuron. Tuning the 2p excitation wavelength slightly changes the transverse position of the 2p image (~one micron). (c) Ratio of two-photon excited relative fluorescence at various excitation wavelengths and three-photon excited relative fluorescence at 1310-nm excitation wavelength. Each ratio and its variation are calculated from the recorded 2P and 3P traces over 210 – 350 seconds.

From our data when there is no transients registered, we can determine the relative background fluorescence of the same neuron as a function of the excitation wavelength after

Biomedical Optics EXPRESS

correcting for the different excitation power and pulse width. In Fig. 5 we show 3p background fluorescence for different excitation wavelength, $F_0(\lambda)$, relative to the background fluorescence at 1275 nm, F_0(1275nm). Figure 5 provides a measure of the 3P relative action cross section of GCaMP6s *in vivo*.

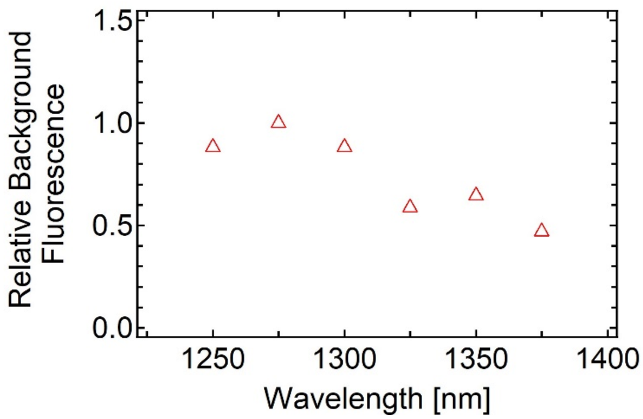

Fig. 5. Background Fluorescence, $F_0(\lambda)$, measured *in vivo* at different excitation wavelengths relative to the background fluorescence at 1275-nm excitation, $F_0(1275nm)$.

4. Discussion

We developed a technique that allows for *in vivo* quantitative measurements of ΔF/F at various wavelengths for 2p and 3p excitation. The objective of this study is to find the optimum excitation condition that allows activity imaging with high fidelity and low excitation power. The ΔF/F needs to be considered in the context of tissue properties (mostly absorption since scattering is relatively constant within the tuning range), imaging depth, and the action cross section, which will all affect the power level needed or allowed to distinguish the transients in the fluorescence traces.

The goal is to use as little excitation power as possible and still have good recording fidelity that allows to distinguish small individual fluorescence transients. To quantify further, we use the pulse discriminatory index [21] that is defined as:

$$d' = \frac{\Delta F}{F_0}\sqrt{F_0 \tau} = \frac{\Delta F}{F_0}\sqrt{C P_{focus}^3 \sigma_\lambda \tau}, \quad (1)$$

where F_0 is the time independent background fluorescence, C is a proportionality constant, P_{focus} is the power at the focus, σ_λ is the 3P action cross section of GCaMP6s, and τ is the decay time constant of the sensor.

In Fig. 6, we show the power on the brain surface necessary to achieve the same pulse discrimination index for different excitation wavelengths relative to the power used at 1325-nm excitation for various imaging depths.

Biomedical Optics EXPRESS

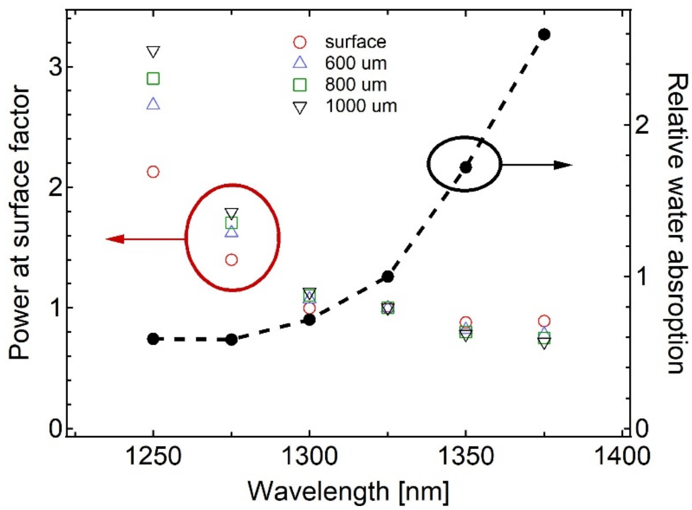

Fig. 6. Excitation power at the surface of the brain required to achieve the same pulse discrimination index at various imaging depths, all normalized to the excitation power at 1325 nm. Relative water absorption normalized to the absorption coefficient at 1325 nm.

Although the highest ΔF/F is at 1375 nm (Fig. 3) and the smaller tissue attenuation at the longer wavelength results in less power required at the surface, tissue absorption (mainly due to water absorption within the wavelength window of 1300 nm) is significantly higher at 1375 nm than at 1300 nm (Fig. 6). Sample heating should be considered in practical imaging experiments. We compare the pulse discrimination index for different excitation wavelengths relative to that at 1300 nm at imaging depth of 1000 μm using the assumption that the maximum permissible power is proportional to tissue absorption length (i.e., proportional to the water absorption length). The results are plotted in Fig. 7, indicating that the wavelength of 1300 nm is optimum. We caution that Fig. 7 somewhat overestimates the relative pulse discrimination index at the shorter wavelength and underestimates at the longer wavelength since the maximum permissible power depends sub-linearly with the absorption length if heat dissipation and heat loss (e.g., through the cranial window) are considered. If shorter pulses with larger bandwidth are used for excitation, averaging over the entire spectral bandwidth of the excitation will need to be performed to calculate the ΔF/F using the measurement data in Fig. 3.

Biomedical Optics EXPRESS

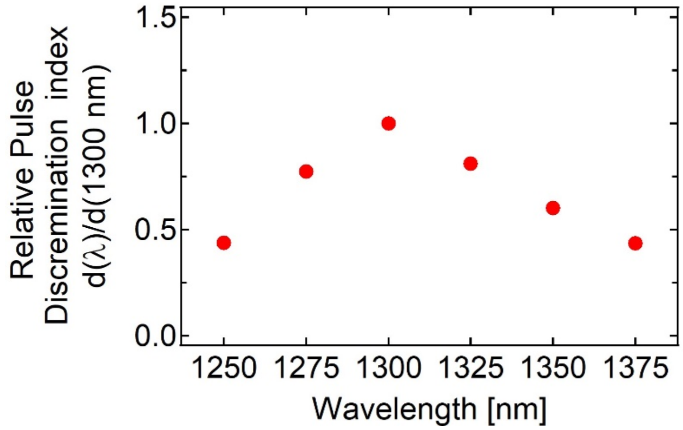

Fig. 7. Pulse discrimination index at imaging depth of 1000 μm when using maximum allowable power at the surface of the brain for different wavelengths, normalized to the pulse discrimination index at 1300 nm.

For 2p excitation within the 880-950 nm region, the tissue absorption and scattering are relatively constant [22]. Therefore, the optimal excitation wavelength is mostly determined by the ΔF/F. Our results confirm that 920-930 nm is the optimum excitation wavelength for 2P *in vivo* imaging of GCaMP6.

5. Conclusion

A TDM 2p and 3p technique has been used to investigate ΔF/F dependence on the excitation wavelength for *in vivo* imaging of GCaMP6s. By using one of the two beams as a reference and varying the wavelength of the second beam, we are able to determine precisely the wavelength dependence of ΔF/F in a live mouse brain. Considering the tissue absorption and GCaMP6s action cross section, we found that the optimal wavelength for 3PM of brain activity is around 1300 nm. For 2PM, the optimal wavelength is around 920-930 nm.

Funding

National Science Foundation (DBI-1707312) NeuroNex.

Acknowledgments

The authors thank members of Xu research group and John Macklin for valuable discussions and technical suggestions.

Disclosures

The authors declare that there are no conflicts of interest related to this article.

References

1. W. Yang and R. Yuste, “In vivo imaging of neural activity,” Nat. Methods **14**(4), 349–359 (2017).
2. D. Smetters, A. Majewska, and R. Yuste, “Detecting action potentials in neuronal populations with calcium imaging,” Methods **18**(2), 215–221 (1999).
3. W. Denk, J. H. Strickler, and W. W. Webb, “Two-photon laser scanning fluorescence microscopy,” Science **248**(4951), 73–76 (1990).
4. W. R. Zipfel, R. M. Williams, and W. W. Webb, “Non-linear magic,” Nat. Biotechnol. **21**, 1369–1377 (2003).
5. C. Stosiek, O. Garaschuk, K. Holthoff, and A. Konnerth, “In vivo two-photon calcium imaging of neuronal networks,” Proc. Natl. Acad. Sci. U.S.A. **100**(12), 7319–7324 (2003).
6. J. N. Kerr and W. Denk, “Imaging in vivo: watching the brain in action,” Nat. Rev. Neurosci. **9**(3), 195–205 (2008).
7. D. A. Dombeck, A. N. Khabbaz, F. Collman, T. L. Adelman, and D. W. Tank, “Imaging large-scale neural activity with cellular resolution in awake, mobile mice,” Neuron **56**(1), 43–57 (2007).

Biomedical Optics EXPRESS

8. T. R. Sato, N. W. Gray, Z. F. Mainen, and K. Svoboda, "The functional microarchitecture of the mouse barrel cortex," PLoS Biol. **5**(7), e189 (2007).
9. W. Mittmann, D. J. Wallace, U. Czubayko, J. T. Herb, A. T. Schaefer, L. L. Looger, W. Denk, and J. N. Kerr, "Two-photon calcium imaging of evoked activity from L5 somatosensory neurons in vivo," Nat. Neurosci. **14**(8), 1089–1093 (2011).
10. D. A. Dombeck, C. D. Harvey, L. Tian, L. L. Looger, and D. W. Tank, "Functional imaging of hippocampal place cells at cellular resolution during virtual navigation," Nat. Neurosci. **13**(11), 1433–1440 (2010).
11. N. G. Horton, K. Wang, D. Kobat, C. G. Clark, F. W. Wise, C. B. Schaffer, and C. Xu, "*In vivo* three-photon microscopy of subcortical structures within an intact mouse brain," Nat. Photonics **7**(3), 205–209 (2013).
12. D. G. Ouzounov, T. Wang, M. Wang, D. D. Feng, N. G. Horton, J. C. Cruz-Hernández, Y. T. Cheng, J. Reimer, A. S. Tolias, N. Nishimura, and C. Xu, "*In vivo* three-photon imaging of activity of GCaMP6-labeled neurons deep in intact mouse brain," Nat. Methods **14**(4), 388–390 (2017).
13. T. Wang, D. G. Ouzounov, C. Wu, N. G. Horton, B. Zhang, C. H. Wu, Y. Zhang, M. J. Schnitzer, and C. Xu, "Three-photon imaging of mouse brain structure and function through the intact skull," Nat. Methods **15**(10), 789–792 (2018).
14. S. Weisenburger, F. Tejera, J. Demas, B. Chen, J. Manley, F. T. Sparks, F. Martínez Traub, T. Daigle, H. Zeng, A. Losonczy, and A. Vaziri, "Volumetric Ca^{2+} Imaging in the Mouse Brain Using Hybrid Multiplexed Sculpted Light Microscopy," Cell **177**(4), 1050–1066 (2019).
15. T. W. Chen, T. J. Wardill, Y. Sun, S. R. Pulver, S. L. Renninger, A. Baohan, E. R. Schreiter, R. A. Kerr, M. B. Orger, V. Jayaraman, L. L. Looger, K. Svoboda, and D. S. Kim, "Ultrasensitive fluorescent proteins for imaging neuronal activity," Nature **499**(7458), 295–300 (2013).
16. H. Dana, B. Mohar, Y. Sun, S. Narayan, A. Gordus, J. P. Hasseman, G. Tsegaye, G. T. Holt, A. Hu, D. Walpita, R. Patel, J. J. Macklin, C. I. Bargmann, M. B. Ahrens, E. R. Schreiter, V. Jayaraman, L. L. Looger, K. Svoboda, and D. S. Kim, "Sensitive red protein calcium indicators for imaging neural activity," eLife **5**(5), e12727 (2016).
17. C. Grienberger and A. Konnerth, "Imaging Calcium in Neurons," Neuron **73**(5), 862–885 (2012).
18. L. M. Barnett, T. E. Hughes, and M. Drobizhev, "Deciphering the molecular mechanism responsible for GCaMP6m's Ca2+-dependent change in fluorescence," PLoS One **12**(2), e0170934 (2017).
19. C. Xu, W. Zipfel, J. B. Shear, R. M. Williams, and W. W. Webb, "Multiphoton fluorescence excitation: New spectral windows for biological nonlinear microscopy," Proc. Natl. Acad. Sci. U.S.A. **93**(20), 10763–10768 (1996).
20. X. Deng, Z. Zhuang, H. Liu, P. Qiu, and K. Wang, "Measurement of 3-photon excitation and emission spectra and verification of Kasha's rule for selected fluorescent proteins excited at the 1700-nm window," Opt. Express **27**(9), 12723–12731 (2019).
21. B. A. Wilt, J. E. Fitzgerald, and M. J. Schnitzer, "Photon Shot Noise Limits on Optical Detection of Neuronal Spikes and Estimation of Spike Timing," Biophys. J. **104**(1), 51–62 (2013).
22. M. Wang, C. Wu, D. Sinefeld, B. Li, F. Xia, and C. Xu, "Comparing the effective attenuation lengths for long wavelength *in vivo* imaging of the mouse brain," Biomed. Opt. Express **9**(8), 3534–3543 (2018).